ISSN: 2447-3359

REVISTA DE GEOCIÊNCIAS DO NORDESTE

Northeast Geosciences Journal

v. 11, nº 1 (2025)

https://doi.org/10.21680/2447-3359.2025v11n1ID36762

Determination of the vertical refractive index, using reciprocal and simultaneous views : analysis of its application in calculating the unevenness using trigonometric leveling

Determinação do índice de refração vertical, utilizando visadas reciprocas e simultâneas: análise de sua aplicação no cálculo do desnível utilizando nivelamento trigonométrico

Dayane Wiggers[1]; Pedro Luis Faggion[2]; Wander da Cruz[3]; Samir de Souza Oliveira Alves[4]

[1] Federal University of Paraná / Department of Geomatics, Curitiba/PR, Brazil. Email: dayane@ufpr.br
ORCID: https://orcid.org/0000-0001-7339-9436

[2] Federal University of Paraná / Department of Geomatics, Curitiba/PR, Brazil. Email: dayane@ufpr.br
ORCID D: https://orcid.org/0000-0002-4881-8720

[3] Federal University of Paraná / Department of Geomatics, Curitiba/PR, Brazil. Email: dayane@ufpr.br
ORCID D: https://orcid.org/0000-0003-0738-1283

[4] State University of Rio de Janeiro / Department of Cartographic Engineering, Rio de Janeiro/RJ, Brazil. Email: samir.alves@eng.uerj.br
ORCID: https://orcid.org/0000-0003-3083-0681

Abstract: The safety and operational efficiency of dams are crucial aspects for their use. However, monitoring these structures faces several challenges. In the context of dam monitoring, the use of total stations has been a practice for controlling the movement of monitoring points. However, atmospheric refraction can introduce significant errors into the measurements performed, affecting the accuracy and reliability of the results. With this in mind, in this work a study was carried out at the hydroelectric power generation plant called Jayme Canet Junior, to analyze the effects of atmospheric refraction in determining unevenness, using data obtained by the first order geometric leveling method. Using the trigonometric leveling method equation, the value of the local refractive index was calculated, reciprocally and simultaneously, between three pillars located on the banks of the dam and in three different periods of the day. After this calculation, the behavior of the refractive index was analyzed, its relationship with local atmospheric conditions and the difference in level between pillars P1, P2 and P3 and two monitoring points located on the crest of the dam, called CG01 and CG02. Analyzing the unevenness values obtained through trigonometric leveling, using the calculated refractive index (k), in each period and for each line of sight, it is possible to see that the unevennesses show improvement in most cases compared to k = 0 ,13. However, this same behavior was not observed for the differences in level obtained from Pillar 3 (P3 – CG01; P3 – CG02), located downstream of the dam. It is estimated that this phenomenon occurred due to the high humidity in the area, due to fog, caused by the flow of water through the spillway, which had three gates open.

Keywords: Vertical refractive index; Monitoring of structures; Leveling.

Resumo: A segurança e a eficiência operacional de barragens são aspectos cruciais para sua utilização. No entanto, o monitoramento dessas estruturas enfrenta diversos desafios. No contexto do monitoramento de barragens, a utilização de estações totais tem sido uma prática para o controle do deslocamento de pontos de monitoramento. No entanto, a refração atmosférica pode introduzir erros significativos nas medições realizadas, afetando a precisão e confiabilidade dos resultados. Pensando nisso, neste trabalho foi realizado um estudo na usina hidrelétrica de geração de energia denominada, Jayme Canet Junior, para avaliar como são os efeitos da refração atmosférica na determinação da constante de refração (k), necessária para o cálculo de desníveis utilizando nivelamento trigonométrico, utilizando como referência os desníveis obtidos pelo método de nivelamento geométrico de primeira ordem. A partir da equação do método de nivelamento trigonométrico, calculou-se o valor do índice de refração local, de forma recíproca e simultânea, entre três pilares. Dois situados montante, na margem direita (P1) e na margem esquerda (P2) e um terceiro a jusante. As medições foram realizadas em três períodos distintos do dia. Após os cálculos, analisou-se o comportamento do índice de refração, sua relação com as condições atmosféricas local e nos valores de desnível entre os pilares P1, P2 e P3 e dois pontos de monitoramento situados na crista da barragem, denominados CG01 e CG02. Analisando os valores dos desníveis obtidos através do nivelamento trigonométrico, utilizando o índice de refração (k) calculado, em cada período e para cada linha de visada, é possível perceber que os valores dos desníveis apresentam melhora na maior parte dos casos em comparação com o emprego do valor k = 0,13. Porém, este mesmo comportamento não foi observado para os desníveis obtidos a partir do Pilar 3 (P3 – CG01; P3 – CG02), situado a jusante da barragem. Estima-se que esse fenômeno ocorreu em função da alta umidade do local, devido a névoa, provocada em razão da vazão da água pelo vertedouro, que estava com as três comportas abertas.

Palavras-chave: Índice de refração vertical; Monitoramento de estruturas; Nivelamento.

Received: 26/06/2024; Accepted: 10/03/2025; Published: 08/04/2025.

1. Introduction

The safety and operational efficiency of dams are crucial aspects for their use. However, monitoring these structures faces several challenges. In the context of dam monitoring, the total stations operation has become a common practice for controlling the displacement of monitoring points on these structures. Nevertheless, atmospheric refraction can introduce significant errors in the measurements performed by these instruments, affecting the accuracy and reliability of the results.

Atmospheric refraction is an optical phenomenon that results from the variation in air density due to changes in environmental parameters such as temperature, pressure, and humidity. This causes a deviation in the electromagnetic wave used by the equipment to perform measurements (RUEGER, 1996). This curvature can distort the geometry of the measurements, thereby affecting the coordinate determinations and, consequently, the monitoring of the structure's points.

This phenomenon has been the subject of several studies, including geodesy, and occurs due to the variation in air density, resulting in the bending of light beams as they pass through different layers of the atmosphere (TORGE, 2001). The influence of atmospheric refraction on the structural monitoring such as hydroelectric dams has attracted increasing interest due to several accidents and incidents that have occurred in recent years.

Previous studies have investigated the effects of atmospheric refraction on measurements performed by total stations under various environmental and geographical conditions. For example, research by Shen et al. (2017) demonstrated that atmospheric refraction can cause considerable deviations in distance and direction measurements, especially in regions with abrupt variations in temperature and humidity.

To mitigate the adverse effects of atmospheric refraction in elevation determination using total stations, different approaches have been proposed. A common approach is the mathematical model application to correct the measurements based on local atmospheric conditions. These models consider parameters such as air temperature, pressure, and humidity to calculate the deviations introduced by atmospheric refraction and correct the distance measured.

In summary, understanding and mitigating the atmospheric refraction effects in total station measurements is essential to ensure the safety and operational efficiency. Future research in this area may focus on developing more accurate and effective atmospheric correction models, as well as integrating different monitoring techniques to achieve more reliable results.

In this study, the atmospheric refraction effects were analyzed using elevation data obtained through first-order geometric leveling, with an accuracy better than 1 mm/km. From the equation of the trigonometric leveling method, the local refractive index was calculated at three different times of the day, under varying conditions of temperature, pressure, and humidity. Then, it was analyzed the refractive index behavior and its influence on the elevation differences between the pillars (P1, P2, and P3) and two monitoring points located on the dam crest, named CG01 and CG02.

2. Methodology

2.1 Study Area

The study area is located at the Governador Jayme Canet Júnior Hydroelectric Power Plant, situated between Ortigueira and Telêmaco Borba cities. The plant was formed by the damming of the Tibagi River, in the Salto Mauá region, in the state of Paraná, Brazil. The dam supplies electricity to approximately one million people and is built with roller-compacted concrete, measuring 745 meters in length at the top and 85 meters in maximum height. When operating at its maximum level, the reservoir forms an inundated area of 83.9 km² (WIGGERS et al., 2020).

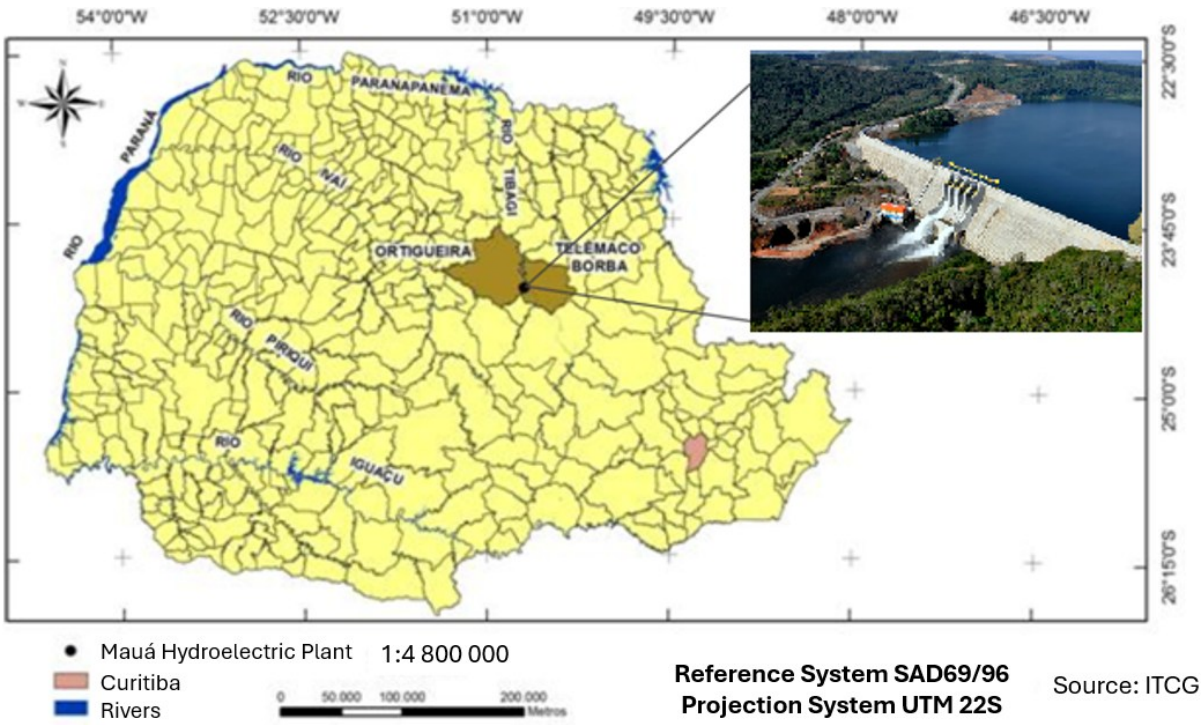

Figure 1 – Location of the study area.
Source: Adapted from Siguel (2013).

2.2 Equipment Used

For measuring horizontal directions, vertical angles, and inclined distances, three total stations were used: two Leica TS15 models and one TCRA 1205 model. These stations have the capability of performing automatic readings through the Automatic Target Recognition (ATR) function, a system that detects prisms quickly and with reduced operator influence.

When used together with the Leica GPR111 prism, the TS15 total stations have an angular measurement accuracy of 3" and 5" and a linear accuracy of 1mm + 1.5ppm (LEICA GEOSYSTEMS, 2015A). The TCRA 1205 total station, on the other hand, has an angular accuracy of 5" and a linear accuracy of 1mm + 1.5ppm (LEICA GEOSYSTEMS, 2015B).

These instruments underwent rigorous verification procedures, using collimators as well as a linear base for calibrating the electronic distance meter (EDM). These calibrations were conducted at the Geodetic Instrumentation Laboratory (*Laboratório de Instrumentação Geodésica* - LAIG) of the Federal University of Paraná (UFPR), where they are also classified to ensure the reliability of the instrument's nominal accuracy.

Along with the total stations, Leica GPR111 prisms were mounted above the instrument's handle, enabling reciprocal and simultaneous observations. Additionally, at points CG01 and CG02, 360º prisms (ZRD121 model) were used.

Figure 2 – Prism installation on the total station handle.
Source: Authors (2024).

The geometric leveling data were collected using the Leica DNA03 digital level, capable of making electronic measurements with a standard deviation of ±0.3 mm/km for double-run leveling, when used with Invar barcode leveling (LEICA GEOSYSTEMS, 2006). During the leveling process, leveling plates were used to ensure that the same point was occupied for both backsight and foresight readings. The height of the leveling screws was measured with a caliper featuring a nominal accuracy of 0.01 mm.

The leveling instrument and staff are periodically calibrated at the Geodetic Instrumentation Laboratory (LAIG). An interferometer is used to establish correction equations for the measurements, ensuring the reliability of the instrument's nominal accuracy. More details can be found in Gemin (2017).

Finally, temperature, atmospheric pressure, and humidity were measured using a portable meteorological station, the Datalogger thermo-hygrometer, with the following measurement accuracies: ±1.5 mbar (pressure), ±1°C (temperature), and ±3% (relative humidity).

2.3 Topographic Survey

On November 13th and 14th, 2023, trigonometric leveling was carried out at three distinct locations: two upstream and one downstream of the dam. The point designated as Pillar 01 is located on the right bank upstream of the dam, Pillar 02 is also upstream on the left bank, and Pillar 03 is situated downstream.

These three pillars were installed even before the dam's construction was completed. To ensure their stability, they were built with foundations reaching the bedrock of the region (SIGUEL, 2013). At the top of each pillar, a forced-centering system with a standard 5/8" screw thread was installed, making them compatible with geodetic equipment. This system ensures that these points can be reoccupied by instruments or prisms at different times. According to Nadal (2000), the estimated reoccupation repeatability using this system is within a tenth of a millimeter.

Figure 3 – Surveyed points (true north).
Source: Adapted from Wiggers et al. (2025).

To enable reciprocal and simultaneous observations, an adapter was developed and attached to the total station's handle to materialize the projection of the instrument's gimbal point. This adapter was designed by the authors through 3D scanning of the handle to determine its dimensions. The part was then modeled using Tinkercad software and subsequently 3D-printed using a Creality CR10 V2 printer. The printed adapter was secured to the total stations' handles with nylon clamps.

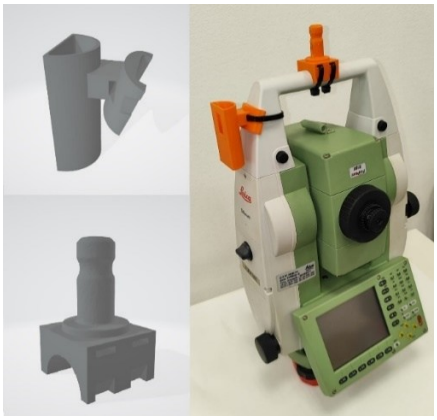

Figure 4 – Support brackets developed for reciprocal observations.
Source: Authors (2024).

The topographic survey involved six series of readings, with direct and inverse telescope pointing (PD, PI). The survey was conducted at three different times: On November 13 in the afternoon, from 3:37 PM to 4:00 PM; On November 14 in the morning, the first session took place from 7:13 am to 7:31 am, and the second session from 10:59 am to 11:14 am. The observations were performed simultaneously between Pillars 01 and 02 and then between 02 and 03. The points CG01 and CG02 were observed from all three pillars simultaneously using 360° prisms. Radio communication was used to synchronize the start of measurements. During the survey, temperature, pressure, and humidity were recorded at each pillar occupied by total stations.

The geometric leveling between the three pillars had been conducted in previous campaigns since the authors are part of a research group that has been monitoring this dam for an extended period. The leveling surveys adhered to all specifications and standards outlined in NBR 13133 (ABNT, 2021) and the General Specifications and Standards for Geodetic Surveys in Brazilian territory (IBGE, 1983). The recorded errors were below the permissible limits in all sections.

For geometric leveling between Pillars 01 and 02, data from the latest campaign in January 2023 were used. The process started at Pillar 02, with the invar staff placed on top of the forced-centering screw (Figure 5). The leveling traverse to Pillar 01 was carried out using auxiliary points materialized with leveling plates, passing through CG01 and CG02, located on the dam crest, and then through Benchmark RN5, positioned next to Pillar 01. The backsight, foresight, foresight, backsight method was applied for elevation difference calculation.

For the leveling between Pillars 01 and 03, only one geometric leveling campaign had been conducted, in July 2019. This survey followed the same methodology described above, concluding with the invar staff placed on the forced-centering screw of Pillar 03. After completion, the screw heights were measured using a caliper with 0.01 mm precision to ensure all elevation differences were referenced to the screw base, the same reference used for trigonometric leveling.

Using the distance between the instrument and the staff, along with the backsight and foresight readings, the elevation difference between two points is determined by subtracting the fore sight reading from the backsight reading. When referencing the forced-centering screw base, two additional terms are introduced in the geometric leveling equation to account for measurements taken above the screws.

Equation 1 – Geometric leveling calculation reduced to the screw base:

$$\Delta H_{AB\ reduced} = L_{backsight} + H_{r\ backsight} - L_{foresight} - H_{r\ foresight}$$

Where: $\Delta H_{AB\ reduced}$ = Elevation difference from A to B reduced to the screw base, $L_{backsight}$ = Backsight reading, $H_{r\ backsight}$ = Screw height at the backsight reading, $L_{foresight}$ = Foresight reading, $H_{r\ foresight}$ = Screw height at the foresight reading.

Figure 5 – Geometric leveling on the forced-centering pillar.
Source: Authors (2024).

2.4 Data Processing

After collecting data with the total station, following the instructions provided in the equipment manual, it is necessary to correct the measured distances due to variations in atmospheric conditions (LEICA GEOSYSTEMS, 2015A). Based on that, atmospheric conditions were recorded at the same time as the measurements using a Datalogger thermo-hygrometer, with data logged at 5-second intervals. The parameters did not vary significantly throughout the survey, so their average values were used.

Table 1 – Variations in Temperature, Pressure, and Humidity

	Pillar 01 - Pillar 02		
	Temperature (°C)	**Pressure (mBar) (mbbçsedk mBar**	**Humidity (%)**
Afternoon	34.0	934.1	59.9
Morning 1	21.6	938.1	91.3
Morning 2	21.6	936.5	70.5
	Pillar 02 - Pillar 01		
Afternoon	29.8	934.2	61.6
Morning 1	22.8	936.6	77.5
Morning 2	22.8	935.0	63.6
	Pillar 02 - Pillar 03		
Afternoon	29.0	934.3	64.8
Morning 1	22.1	936.3	78.5
Morning 2	22.1	935.2	63.9
	Pillar 03 - Pillar 02		
Afternoon	28.4	940.2	73.2
Morning 1	22.8	942.5	88.4
Morning 2	22.8	942.1	76.7

Source: Authors (2024).

By knowing the pressure, humidity, and temperature conditions measured during the survey, it is possible to correct the values of the measured inclined distances (LEICA GEOSYSTEMS, 2015A; LEICA GEOSYSTEMS, 2015B):

Equation 2 Atmospheric Correction for TS15:

$$\Delta D = 286{,}338 - \left[\frac{0{,}29535p}{1+\alpha t} - \frac{4{,}126.10^{-4}h}{1+\alpha t}.10^{x}\right]$$

Equation 3 Atmospheric Correction for TCRA1205:

$$\Delta D = 286{,}34 - \left[\frac{0{,}29525p}{1+\alpha t} - \frac{4{,}126.10^{-4}h}{1+\alpha t}.10^{x}\right]$$

Where: ΔD = Atmospheric correction in PPM, p = Pressure in mbar or hPa, t = Temperature in °C, h = Air humidity in %, α = 1/273,15 e $x = \left(\frac{7{,}5\,t}{237{,}3+t}\right) + 0{,}7857$.

The corrections for inclined distances were performed using Excel software. Once the corrected inclined distances and measured vertical angles were obtained, the vertical and horizontal distance components were calculated.

Using the equation for determining height differences through trigonometric leveling, it is possible to rearrange it to determine the refraction index, given that the height difference (ΔH_{AB}) obtained from geometric leveling is already known.

Equation 4 Trigonometric Height Difference Calculation:

$$\Delta H_{AB} = h_i - h_s + D_v + \frac{D_h^2}{2R} + \frac{kD_h^2}{2R}$$

Where: ΔH_{AB} = Height difference between points A and B, h_i = Instrument height, h_s = Prism height, D_v = Vertical component of the inclined distance, D_h = Horizontal component of the inclined distance, R = Earth's radius, k = Refraction coefficient.

By isolating the term k, which represents the refraction coefficient, the equation can be rewritten to determine its value.

Equation 5 – Vertical Refraction Coefficient Calculation:

$$k = \frac{(2R\Delta H_{AB} + 2Rh_i - 2Rh_s + 2RD_v + D_h^2)}{D_h^2}$$

Where: k = Vertical refraction coefficient, R = Earth's radius, ΔH_{AB} = Height difference between points A and B, h_i = Instrument height, h_s = Prism height, D_v = Vertical component of the inclined distance, D_h = Horizontal component of the inclined distance.

3. Results and Discussion

3.1 Geometric Leveling

The elevation differences between the pillars and points CG01 and CG02, as previously described and reduced to the base of the screw, are presented in table 2.

Table 2 – Geometric Elevation Differences Between Points.

Survey Line	Elevation Difference (m)
Pillar01 - Pillar02	11.2944
Pillar02 - Pillar01	-11.2944
Pillar02 - Pillar03	-65.8658
Pillar03 - Pillar02	65.8658
Pillar01 - CG01	-4.2619
Pillar01 - CGO2	-4.2605
Pillar02 - CG01	-15.5546
Pillar02 - CGO2	-15.5531
Pillar03 - CG01	50.3095
Pillar03 - CGO2	50.3110

Source: Authors (2025).

3.2 Vertical Refraction Index

With the inclined distances already corrected for environmental effects according to equations 2 and 3, the accuracy of the measured distances was analyzed using MED, following NBR 13.133 (ABNT, 2021), resulting in a precision of approximately 1.4 mm. Using equation 5, along with the values of the vertical and horizontal distance components, as well as the instrument and prism heights, the vertical refraction coefficient was calculated for each survey line separately. This calculation was performed for the four sighting lines, at three different periods of the day when the survey was conducted, allowing an evaluation of the vertical refraction index for each line individually. The vertical refraction index could also be calculated using equation 4, where the ΔH_{AB} values, measured reciprocally and simultaneously between the pillars could be considered equal. However, the values obtained through geometric leveling were preferred, as this method ensures greater accuracy and serves as reference.

Table 3 – Instrument and Prism Heights.

HEIGHTS	(mm)
Hi (P1 P2 P3)	236.7
Hs (P1 P2 P3)	466.2
Hs (P2 - P1) morning & noon	469.2
Hs prism	300.0

Source: Authors (2025).

Table 1 – Distance in the afternoon.

CORRECTED DISTANCES	Zenith Angle	Dh (m)	Dv (m)	DI (Uncorrected)	DI (Corrected)
Pillar 01 - Pillar 02	89°7'59"	757.8341	11.4717	757.8890	757.9210
Pillar 02 - Pillar 01	90°50'22"	757.8309	-11.1013	757.8830	757.9122
Pillar 02 - Pillar 03	96°19'18"	592.8706	-65.6834	596.4754	596.4980
Pillar 03 - Pillar 02	83°38'20"	592.8774	66.0854	596.5278	596.5492

Source: Authors (2025).

Table 2 – Distance in the morning 1.

CORRECTED DISTANCES	Zenith Angle	Dh (m)	Dv (m)	DI (Uncorrected)	DI (Corrected)
Pillar 01 - Pillar 02	89°8'4"	757.8304	11.4713	757.8940	757.9172
Pillar 02 - Pillar 01	90°50'22"	757.8363	-11.0925	757.8934	757.9175
Pillar 02 - Pillar 03	96°19'20"	592.8717	-65.6812	596.4802	596.4989
Pillar 03 - Pillar 02	83°38'20"	592.8774	66.0930	596.5319	596.5500

Source: Authors (2025).

Table 3 – Distance in the morning 2.

CORRECTED DISTANCES	Zenith Angle	Dh (m)	Dv (m)	DI (Uncorrected)	DI (Corrected)
Pillar 01 - Pillar 02	89°8'3"	757.8319	11.4746	757.8904	757.9188
Pillar 02 - Pillar 01	90°50'24"	757.8307	-11.1108	757.8836	757.9122
Pillar 02 - Pillar 03	96°19'27"	592.8719	-65.6940	596.4782	596.5005
Pillar 03 - Pillar 02	83°38'20"	592.8783	66.0855	596.5294	596.5500

Source: Authors (2025).

Table 4 – Refraction Index for Each Sight Line.

Sight Line	Period	k
Pillar 01 - Pillar 02	Afternoon	-0.1235
	Morning 1	-0.1329
	Morning 2	-0.0587
Pillar 02 - Pillar 01	Afternoon	0.1505
	Morning 1	0.2784
	Morning 2	-0.1293
Pillar 02 - Pillar 03	Afternoon	-0.7144
	Morning 1	-0.6344
	Morning 2	-1.1013
Pillar 03 - Pillar 02	Afternoon	0.6397
	Morning 1	0.9151
	Morning 2	0.6432

Source: Authors (2025).

It is observed that the k values exhibit very similar behavior for each sighting line. Since the measurements were performed reciprocally and simultaneously, meaning the environmental conditions along the electromagnetic wave path were the same, the vertical refraction index values are close but with opposite signs.

When the medium through which the measurements are taken has variable density, the beam curvature occurs so that it follows the shortest optical path. Therefore, by analyzing the pressure, temperature, and relative humidity values, an approximation of the air density can be made in the region near the pillars, where the environmental parameters were measured.

3.3 Density

To calculate the density value, we would need to consider a series of factors such as air composition, humidity, pollution, and thermodynamic aspects, which, in practice, is quite complex. According to Gill (1982), dry air has a relatively stable composition (78.1% Nitrogen, 21.0% Oxygen, and 0.9% Argon), with the variable factor being the amount of water vapor present in this mixture. According to Petty (2008), water, unlike permanent gases, is constantly changing in the atmosphere. These variations occur primarily due to its evaporation from surfaces and vegetation. Since these processes strongly depend on local conditions, the distribution of water in the atmosphere is highly variable.

Based on Petty's (2008) definition, a mathematical relationship is established for calculating density through approximations derived from the ideal gas law. This method converts the measured temperature into a virtual temperature, which is defined as the temperature that a parcel of dry air would have so that its density equals that of a humid air parcel, assuming the same pressure conditions.

Equation 6 Definition of Virtual Temperature:

$$\mathrm{T}_v = \left[1 + \left(\frac{1}{\varepsilon} - 1\right)\ \mathrm{q}\right] T$$

$$\varepsilon\ = \frac{R_d}{R_v} = 0{,}622$$

$$\mathrm{q}\ \approx w = 0{,}03$$

Where: T_v = Virtual Temperature (K), R_d = Gas constant for dry air, R_v = Gas constant for pure water vapor, w = Ratio between the mass of water vapor and the mass of dry air, T = Temperature (K).

Table 5 – Virtual Temperature for Each Sight Line.

Sight Line	Period	Virtual Temperature (K)
Pillar 01 - Pillar 02	Afternoon	312.7498
	Morning 1	300.1237
	Morning 2	300.1237
Pillar 02 - Pillar 01	Afternoon	308.4732
	Morning 1	301.3456
	Morning 2	301.3456
Pillar 02 - Pillar 03	Afternoon	307.6586
	Morning 1	300.6329
	Morning 2	300.6329
Pillar 03 - Pillar 02	Afternoon	307.0477
	Morning 1	301.3456
	Morning 2	301.3456

Source: Authors (2024).

More details about this definition can be found in Perry (2008).

Knowing the values of virtual temperature, pressure, and the specific constant of dry air, it is possible to calculate the air density value.

Equation 7 Air Density Calculation:

$$\mathrm{p} = \rho\ R_d\ T_v$$

Where: p = Air density, R_d = Specific gas constant for dry air $(287{,}047 J/kg\,K)$, T_v = Virtual temperature (K), p = Pressure (Pa).

Table 6 – Air Density at the Pillar During the Corresponding Sight Line Survey.

Sight Line	Period	Density
Pillar 01 - Pillar 02	Afternoon	1.041
	Morning 1	1.089
	Morning 2	1.087
Pillar 02 - Pillar 01	Afternoon	1.055
	Morning 1	1.083
	Morning 2	1.081
Pillar 02 - Pillar 03	Afternoon	1.058
	Morning 1	1.085
	Morning 2	1.084
Pillar 03 - Pillar 02	Afternoon	1.067
	Morning 1	1.090
	Morning 2	1.089

Source: Authors (2025).

According to Torge (2001), density variation has a direct impact on the propagation speed of the electromagnetic wave used in measurements, which can result in changes in travel time and the curvature of the beam. Since the refractive index is influenced by environmental parameters and, consequently, by the density of the medium, these variations will also affect its value (RÜEGER, 1990).

The relationship between air density and the vertical refractive index is crucial in geodetic surveys, as it influences the accuracy of distance and angle measurements. As air density changes with atmospheric conditions, the refractive index also varies, affecting the trajectory of the electromagnetic wave. In regions with higher density, the refractive index tends to be greater, resulting in a curvature that may distort measurements. Conversely, where air density is lower, the refractive index decreases, potentially introducing errors in coordinate determination.Therefore, to ensure accuracy in geodetic surveys, it is essential to consider these variables and apply appropriate corrections that take local atmospheric conditions into account.

With the refractive index values, it is possible to calculate the elevation differences obtained through trigonometric leveling between Pillars (P1, P2, and P3) and points CG01 and CG02. These elevation differences were calculated using both the computed refractive index values and a fixed refractive index of 0.13 to allow for a comparison between the two approaches.

Table 7 – Elevation Difference via Trigonometric Leveling and Its Differences Compared to Geometric Leveling Between the Pillars and Point CG01.

Line	AFTERNOON			
	Elevation Difference (k = 0.13)	Elevation Difference (k calc)	Difference (m) (k = 0.13) - Geometric	Difference (m) (k calc) - Geometric
Pillar01 - CG01(K=P1-P2)	-4.2667	-4.2653	-0.0048	-0.0033
Pillar02 - CG01(K=P2-P1)	-15.5446	-15.5451	0.0100	0.0095
Pillar02 - CG01(K=P2-P3)	-15.5446	-15.5265	0.0100	0.0280

Pillar03 - CG01(K=P3-P2)	50.3274	50.3274	0..0179	0.0179
Line	**MORNING 1**			
	Elevation Difference (k = 0.13)	**Elevation Difference (k calc)**	**Difference (m) (k = 0.13) - Geometric**	**Difference (m) (k calc) - Geometric**
Pillar01 - CG01(K=P1-P2)	-4.2640	-4.2629	-0.0020	-0.0009
Pillar02 - CG01(K=P2-P1)	-15.5446	-15.5463	0.0100	0.0083
Pillar02 - CG01(K=P2-P3)	-15.5431	-15.5167	0.0115	0.0379
Pillar03 - CG01(K=P3-P2)	50.3263	50.3274	0.0168	0.0179
Line	**MORNING 2**			
	Elevation Difference (k = 0.13)	**Elevation Difference (k calc)**	**Difference (m) (k = 0.13) - Geometric**	**Difference (m) (k calc) - Geometric**
Pillar01 - CG01(K=P1-P2)	-4.2648	-4.2637	-0.0028	-0.0017
Pillar02 - CG01(K=P2-P1)	-15.5449	-15.5393	0.0097	0.0152
Pillar02 - CG01(K=P2-P3)	-15.5449	-15.5185	0.0097	0.0361
Pillar03 - CG01(K=P3-P2)	50.3273	50.3284	0.0178	0.0189

Source: Authors (2025).

Table 11 – Elevation Difference via Trigonometric Leveling and Its Differences Compared to Geometric Leveling Between the Pillars and Point CG02.

Line	**AFTERNOON**			
	Elevation Difference (k = 0.13)	**Elevation Difference (k calc)**	**Difference (m) (k = 0.13) - Geometric**	**Difference (m) (k calc) - Geometric**
Pillar01 - CG02(K=P1-P2)	-4.2725	-4.2730	-0.0121	-0.0126
Pillar02 - CG02(K=P2-P1)	-15.5459	-15.5459	0.0073	0.0072
Pillar02 - CG02(K=P2-P3)	-15.5459	-15.5477	0.0073	0.0054
Pillar03 - CG02(K=P3-P2)	50.3294	50.3229	0.0184	0.0119
Line	**MORNING 1**			
	Elevation Difference (k = 0.13)	**Elevation Difference (k calc)**	**Difference (m) (k = 0.13) - Geometric**	**Difference (m) (k calc) - Geometric**
Pillar01 - CG02(K=P1-P2)	-4.2667	-4.2602	-0.0063	0.0003
Pillar02 - CG02(K=P2-P1)	-15.5459	-15.5514	0.0073	0.0017

Pillar02 - CG02(K=P2-P3)	-15.5509	-15.5527	0.0022	0.0004
Pillar03 - CG02(K=P3-P2)	50.3281	50.3323	0.0171	0.0214
Line	**MORNING 2**			
	Elevation Difference (k = 0.13)	**Elevation Difference (k calc)**	**Difference (m) (k = 0.13) - Geometric**	**Difference (m) (k calc) - Geometric**
Pillar01 - CG02(K=P1-P2)	-4.2651	-4.2586	-0.0046	0.0019
Pillar02 - CG02(K=P2-P1)	-15.5511	-15.5502	0.0020	0.0029
Pillar02 - CG02(K=P2-P3)	-15.5511	-15.5529	0.0020	0.0002
Pillar03 - CG02(K=P3-P2)	50.3290	50.3333	0.0181	0.0223

Source: Authors (2024).

To evaluate the consistency of the results, a statistical analysis was conducted on the elevation differences obtained using trigonometric leveling between the pillars and points CG01 and CG02. The analysis considered the vertical refraction index, calculated through reciprocal and simultaneous sightings, and a refraction index of k = 0.13. A hypothesis test was employed to determine whether the elevation differences obtained through trigonometric leveling using k = 0.13 and the calculated k were equal to those obtained through geometric leveling. The null hypothesis states that the values are equal, while the alternative hypothesis states that they are different.

- Null hypothesis: H_0: $\Delta H_{trigonometric} = \Delta H_{geometric}$
- Alternative hypothesis: H_a: $\Delta H_{trigonometric} \neq \Delta H_{geometric}$

To evaluate the hypotheses, Student's t-distribution was used. According to Gemael, Machado, and Wandresen (2015), this distribution is recommended for samples with fewer than 30 elements.

Equation 8 Student's t-distribution

$$T = \frac{\overline{\Delta H_{\,trigonometric}} - \overline{\Delta H_{\,geometric}}}{\sqrt{\frac{s^2}{v} + \frac{s^2}{v}}}$$

Where: T = Student's t-distribution; $\overline{\Delta H_{\,trigonometric}}$ = Mean elevation difference obtained via trigonometric leveling (using either k = calculated or k = 0.13); $\overline{\Delta H_{\,geometric}}$ = Mean elevation difference obtained via geometric leveling; s = Standard deviation of the mean; v = Degrees of freedom.

A 95% confidence level was used (significance level of 5%). With two degrees of freedom, the critical value from the Student's t-table is 2.920. Thus, the null hypothesis is accepted for test values between -2.920 and 2.920.

For the elevation differences obtained from the trigonometric leveling of pillars P1, P2, and P3 to CG01 and CG02 using k = 0.13, the alternative hypothesis is true since the values fall outside the critical threshold. Therefore, these values are statistically different from those obtained through geometric leveling.

For the trigonometric leveling from Pillar 01 to CG01, when employing the calculated refraction index based on the sighting from Pillar 01 to Pillar 02, it is statistically considered equal to the geometric leveling, meaning the null hypothesis is true.

Similarly, the trigonometric leveling from Pillar 01 to CG02, using the calculated k from the sighting from Pillar 01 to Pillar 02, is also statistically classified as equal to the geometric leveling.

The elevation difference from Pillar 02 to CG02, applying the calculated refraction index from the sighting from Pillar 02 to Pillar 01, also yields statistically equal results, confirming the null hypothesis. For all other combinations, the null hypothesis is false, meaning the elevation differences are not considered equal.

4. Final Considerations

By analyzing these data and understanding the behavior of the refraction index and density variation, it is possible to observe that most of the presented values align with the physical principles of geometric optics. According to these principles, when an electromagnetic wave travels through a medium with an increasing refraction index along its path, the beam deviates toward the optical axis, causing a variation between the measured elevation difference (using trigonometric leveling) and the reference elevation difference (based on geometric leveling values).

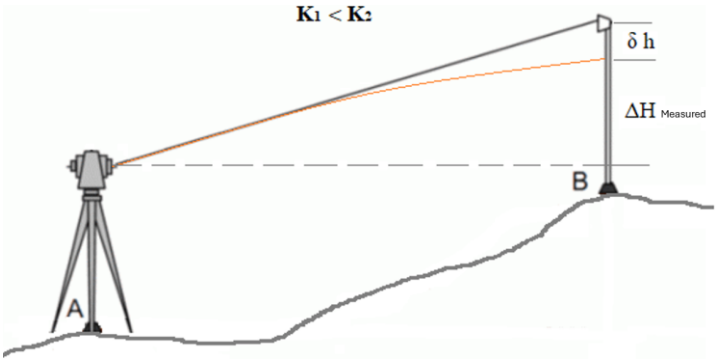

Figure 6 – Deviation of a wave through a medium with a lower refraction index to a medium with a higher refraction index.
Source: Authors (2025).

In this case, the measured elevation difference will be lower than the reference value.
Equation 9 Elevation difference variation when $K_1 < K_2$:

$$\Delta H_{AB\ Reference} = \Delta H_{AB\ Measured} + \delta h$$

Where: $\Delta H_{AB\ Reference}$ = Reference elevation difference from A to B, obtained through geometric leveling, $\Delta H_{AB\ Measured}$ = Elevation difference obtained through trigonometric leveling from A to B, δh = Deviation introduced due to beam curvature.

Similarly, if an electromagnetic wave travels from a medium with a higher refraction index to a medium with a lower refraction index (meaning that the refraction index decreases along the wave's path), the wave deviates away from the optical axis.

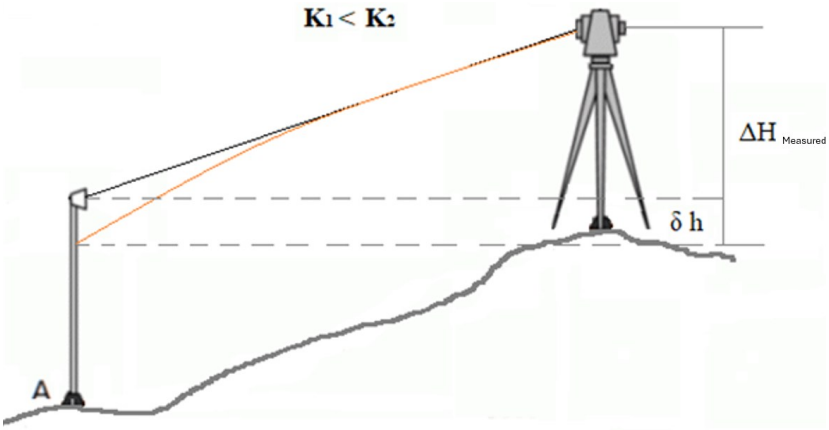

Figure 3 – Deviation of a wave through a medium with a higher refraction index to a medium with a lower refraction index.

Source: Authors (2025).

In this case, the measured elevation difference will be greater than the reference value.

Equation 10 Elevation difference variation when $K_1 < K_2$:

$$\Delta H_{BA\ Reference} = \Delta H_{BA\ Measured} - \delta h$$

Where: $\Delta H_{BA\ Reference}$ = Reference elevation difference from B to A, obtained through geometric leveling, $\Delta H_{BA\ Measured}$ = Elevation difference obtained through trigonometric leveling from B to A, δh = Deviation introduced due to beam curvature.

This behavior can be observed in all sightlines between P2 and P3. At P3, the densities are higher, and consequently, the refraction index is also greater than at P2. As a result, the electromagnetic wave deviates, leading to a measured elevation difference greater than the reference value when measured from P3, and a lower elevation difference than the reference when measured from P2.

For the sightlines between Pillars 01 and 02, the behavior was slightly different. In the afternoon, the trend followed the previously described pattern. However, discrepancies were observed during the morning measurements. In the first morning period, density decreased while the refraction coefficient increased, which may be explained by atmospheric condition variations between points being nearly within the precision range of the equipment, potentially affecting the density calculation.

During the second morning period, density values also decreased, but the refraction index values were both negative, with a variation amplitude of approximately 0.1234.

Another notable detail is that, even after applying the manufacturer's suggested corrections for environmental effects, discrepancies in inclined distance measurements can still be observed, reaching up to 6.5 mm depending on the time of day. Considering that the measured distances are less than 1 km, this discrepancy exceeds the nominal precision of the instrument. As described by Rueger (1996), due to the quality of the refraction index, there is an inherent limitation in the precision of the electronic distance meter.

Analyzing the elevation differences obtained through trigonometric leveling with the calculated refraction index, for each period of the day and each line of sight, it was observed that out of the 22 combinations of elevation differences between the pillars (P1, P2, and P3) and points CG01 and CG02, in 13 cases, using the calculated refraction index improved the difference between the reference and measured elevations, one case showed no change, and in 10 cases, the results worsened when compared to the trigonometric leveling with k=0.13.

Thereby, looking at these 10 cases where discrepancies increased, 8 involved the calculated refraction index from sightlines between P2 and P3. Since this sightline was affected by mist due to the opening of the spillway, this could be a justification for the worsened results.

For leveling between Pillar 01 and CG01, it can be concluded that using the calculated refraction index from the sightline of P1 to P2 always improves the trigonometric leveling results. Similarly, for leveling between Pillar 02 and CG02, the results always improve when using the refraction index calculated from the sightline of P2 to P3.

Statistical analysis using the Student's t-test demonstrated that the elevation difference from Pillar 01 to CG01 can be considered equal to the reference elevation when using the calculated k from the sightline of Pillar 01 to Pillar 02.

As well as the elevation difference between Pillar 01 and CG02 is statistically equal when using the calculated k from the sightline of Pillar 01 to Pillar 02.

The elevation difference from Pillar 02 to CG02, applying the calculated k from the sightline of Pillar 02 to Pillar 01, is also considered equal to the reference, meaning the null hypothesis is true. All other combinations using either the calculated k or k=0.13 are statistically different from the reference elevation, meaning they are false for the null hypothesis.

The refraction index data obtained between Pillar 02 and Pillar 03 showed errors of approximately 18 mm, suggesting that the sightline, being affected by the open spillway, influenced the error caused by atmospheric refraction effects.

Therefore, further studies are necessary to analyze atmospheric behavior along the entire measurement path, enabling a better evaluation of air density variations and their influence on the deviation of the electromagnetic wave used by the instrument.

The data obtained from the between Abutment 02 and Abutment 03 showed errors of around 18 mm, which suggests that the line of sight, because the spillway was open, influenced the error caused by atmospheric refraction.

Acknowledgments

We thank the post-graduation program in Geodesic Sciences for the opportunity to conduct this research and COPEL for providing the study area.

Referencies

ABNT - Associação Brasileira de Normas Técnicas. NBR 13133: Execução do levantamento topográfico – Procedimento. Rio de Janeiro: ABNT, 2021.

COPEL - Companhia Paranaense de Energia. Geração. 2021. Disponível em: http://www.consorciocruzeirodosul.com.br/a-usina. Acesso em: 20 out. 2021.

Gemael, C.; Machado, A. M. L.; Wandresen, R. *Introdução ao ajustamento de observações: aplicações geodésicas*. 2. ed. Ed. UFPR. 2015. 428p.

Gill, A. E. **Atmosphere – Ocean Dinamics**. Academic Press, 1982. 662p.

IBGE - Instituto Brasileiro de Geografia e estatística. Especificações e Normas Gerais para Levantamentos Geodésicos em território brasileiro. Rio de Janeiro: IBGE, 1983.

LEICA GEOSYSTEMS A. Leica 1205. *Manual de operação, versão 3.0, espanhol*. 2015.

LEICA GEOSYSTEMS B. Leica TS15. *Manual de operação, versão 3.0, espanhol*. 2015.

GEMIN, A. R. S. *Desenvolvimento de um sistema de calibração horizontal para sistemas de nivelamento digitais.* Curitiba, 2017. 135f. Tese (Doutorado em Ciências Geodésicas). Programa de Pós-Graduação em Ciências Geodésicas, Universidade Federal do Paraná, Curitiba-PR, 2017.

NADAL, C. A. *Método da inserção óptica tridimensional aplicado à engenharia de precisão*. Curitiba, 2000. 116f. Tese (Doutorado em Ciências Geodésicas). Programa de Pós-Graduação em Ciências Geodésicas, Universidade Federal do Paraná, Curitiba-PR, 2000.

Petty, G. W. **A First Course in Atmospheric Thermodynamics.** Sundog Pub, 2008. 337p.

Rueger, J. M. **Electronic Distance Measurement: An introduction**. 4 ed. Berlin: Springer, 1996.

Shen, Y. Huang, T. Guo, X. Zang, Huerta, Q. M. H. Inversion Method of Atmospheric Refraction Coefficient based on Trigonometric Leveling Network. **Jornal of Surveying Engeneering**, v. 143 (1), 2017.

SIGUEL, A. R. *Monitoramento da Barragem da Usina Hidrelétrica Mauá Utilizando Irradiação Tridimensional*. Curitiba, 2013. 171f. Dissertação (Mestrado em Ciências Geodésicas). Programa de Pós-Graduação em Ciências Geodésicas, Universidade Federal do Paraná, Curitiba-PR, 2013.

Torge, W. **Geodesy**. 3 ed. Walter de Gruyter: Berlin, 2001.

Wiggers, D. Faggion, P. L. Da Cruz, W. Análise do Índice de Refração Vertical no Monitoramento de Barragens: Estudo de Caso UHE Governador Jayme Canet Junior. **Anuário de Geociências**, v. 43 n. 3, 2020.